Line Detection and Texture Characterization of Network Patterns

Costantino Grana, Rita Cucchiara
Department of Information Engineering
University of Modena and Reggio Emilia
{grana.costantino,cucchiara.rita}@unimore.it

Giovanni Pellacani, Stefania Seidenari
Department of Dermatology
University of Modena and Reggio Emilia
{pellacani.giovanni,seidenari}@unimore.it

Abstract

This paper describes a complete approach to detect, localize and describe network patterns. Such texture is automatically detected with Gaussian derivative kernels and Fisher linear discriminant analysis; line closure and thinning is provided by morphological masking and line luminance profile fitting provides width estimation. Detection results on dermatological images are reported and discussed.

1. Introduction

In this work, the problem of line detection, closure, thinning and texture characterization of images with network patterns is addressed. Many natural images in fact contain network like patterns, such as SAR landscapes, solar or medical images (heart physiology or dermatological conditions). This is a typical problem of non-uniform texture analysis, where edge detection cannot provide effective results by itself. Some approaches propose a global analysis of the textures in partitions of the image, such as with co-occurrence matrices, or wavelet transform, which characterize an area, but do not provide precise localization of the pattern within it [1]. A seminal work on linear structure identification is [2], which was applied on road detection and dermatological images [3].

In this paper, we will start from this important theoretical work, and address several open issues found in many actual cases, such as line threshold selection, closure on junction points and network features to quantify the network characteristics. The application is tested on dermatological melanocytic lesion images. A set of specific patterns have been described in literature, and clear significance of these structural characteristics (dots, dark globules and lesion network) has been observed [3]. The lesion network in particular is highly rated as a diagnostic parameter, especially if network line width and network distribution are taken into account.

2. Line points detection

For line points detection we employed the approach described in [2], which works on gray level images. The image is regarded as a surface in which the pixel luminance value is the surface's height. In this approach, the lines are ridges and can thus be identified as the sets of points which satisfy at the same time two conditions on the first and second order derivatives, in the direction orthogonal to the line. The first order derivative should be zero, while the second order derivative should give a high module value. The line's direction, and thus its normal, can be obtained from the Hessian matrix:

$$H(x,y)=\begin{pmatrix} r_{xx} & r_{xy} \\ r_{xy} & r_{yy} \end{pmatrix} \quad (1)$$

where r_{xx}, r_{xy}, r_{yy} are the second order partial derivatives of the image. These are obtained by the convolution with bidimensional kernels computed by the direct discretization of the continuous function. These kernels approximate Gaussian functions whose standard deviation σ is directly tied to the expected line width, and in particular the detection condition is $\sigma \geq w/\sqrt{3}$. This inequality guarantees that the second derivative response has a single minimum in case of light lines on dark background and a single maximum in case of dark lines on light background, which is well defined in case of point in which the first derivatives is zero.

To determine if the first derivative in the orthogonal direction has a zero point within the current pixel, we employ a quadratic Taylor polynomial:

$$p(x)=r+r'x+\frac{1}{2}r''x^2 \quad (2)$$

where r, r', r'' are the derivatives estimated by convolving the image respectively with the Gaussian kernel, the first order deirivative, and second order derivative of the Gaussian kernel.

This function provides an estimate of the behavior of the filtered image in the direction perpendicular to the line and allows also a subpixel precision positioning. But how do

we obtain the exact zero solution? The point in which $p'(x)=0$ is given by

$$x=-\frac{r'}{r''} \tag{3}$$

If we call (n_x,n_y) the vector with unity norm, pointing in the direction orthogonal to the line in the pixel with coordinates (x,y) and if we call $x=(p_x,p_y)$, with $(p_x,p_y)=(tn_x,tn_y)$, the previous equation may be written as:

$$t=-\frac{r_x n_x+r_y n_y}{r_{xx}n_x^2+2r_{xy}n_x n_y+r_{yy}n_y^2} \tag{4}$$

where r_x, r_y, r_{xx}, r_{xy}, r_{yy} are the image partial derivatives, as before. Given a coordinate system centered in the current pixel, this is a line point if:

$$(p_x,p_y)\in\left[-\frac{1}{2},+\frac{1}{2}\right]\times\left[-\frac{1}{2},+\frac{1}{2}\right] \tag{5}$$

Of all the points which satisfy this condition, the significant ones are those in which the maximum module eigenvalue of the Hessian matrix is high.

To provide an automatic selection for the eigenvalue threshold we use the Fisher linear discriminant analysis [4], analyzing the full set of eigenvalues obtained. The maximum module eigenvalue at each point may be either positive or negative, corresponding respectively to dark curvilinear structures on a bright background or vice versa. The negative values should be taken into account, since in a lesion with a network pattern these eigenvalues should present minima of the same magnitude of the positive ones. This is due to the fact that curvilinear structures found in the mash have comparable intensity to the network lines which surround it.

The Fisher technique is used to identify the threshold value λ_{th} which, maximizing the ratio between the interclass and intraclass dispersion, allows to divide the set of values into two well separated classes. The interclass dispersion is given by the squared difference between the two classes averages, the intraclass dispersion by the sum of the two classes variances, so the value to be maximized is

$$J(i)=\frac{\left|a_1(i)-a_2(i)\right|^2}{s_1^2(i)+s_2^2(i)},\ i=1\ldots n \tag{6}$$

where $a_1(i)$ and $a_2(i)$ are the two class averages and $s_1^2(i)$ and $s_2^2(i)$ are the corresponding variances.

3. Line closure

The set of line points obtained with the algorithm described above is neither complete nor closed: a closing process is needed. In [2], in order to close the lines, Steger proposes the use of some of the information already available from the previous step, such as the perpendicular direction $(n_x,n_y)=(\cos\alpha,\sin\alpha)$, the line strength (second order derivative along α), and the subpixel localization of the line points (p_x,p_y). For each extreme point, a 3-point oriented neighborhood is checked to minimize the sum $d+\beta$, where

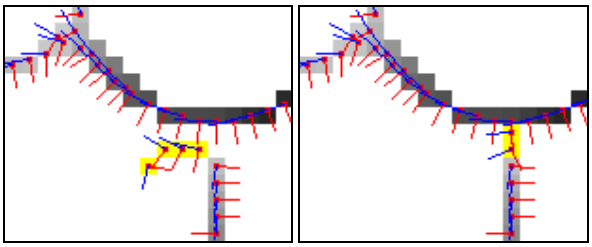

Figure 1. Error in line closing and morphological correction.

$$d=\left\|p_2-p_1\right\|_2 \tag{7}$$

$$\beta=\left|\alpha_2-\alpha_1\right|,\beta\in\left[0,\frac{\pi}{2}\right] \tag{8}$$

represent respectively the distance between the two points and the angular direction between the straights orthogonal to the line in the considered points. Unfortunately, this approach, which seems promising with ideal images, does not cope with the main problem in junction points, which are all those points in which one of the previous conditions is not satisfied: the direction deviates from the real line. In particular, at junction points the *weaker* line (the line with less contrast) gets parallel to the stronger one. In this case the algorithm often follows the stronger line failing to close the gap, even in case of small distances, producing parallel extensions of the lines. An example of this error is shown in Fig. 1.

Our solution begins with a first operation to find the line terminations with morphological masking. Therefore we employ a set of masks, such as those in Fig. 2. These masks are then rotated in the other three directions, in order to identify all these kind of terminations.

Every termination is characterized by a weighting factor, controlled by the number of pixels connected to it. This weight controls the amount of extension allowable for that termination. The extension is done in the direction of the line, as identified by the Hessian matrix, and is implemented at pixel level using the Bresenham algorithm [5]. If this extension is within the lesion boundaries and reaches

0	0	0
0	T	N
0	0	0

0	0	0
0	T	N
0	0	N

0	0	N
0	T	N
0	0	0

0	0	N
0	T	N
0	0	N

Figure 2. Morphological masks for network terminations search. T is the termination point, while N is a network point.

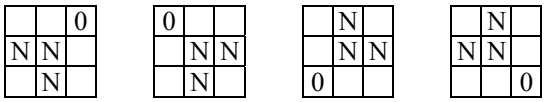

Figure 4. Exclusive morphological masks for network thinning at "L" points. N is a network point, 0 is a non-network point, while empty elements are ignored.

another network element, it is confirmed and added to the network. Whether the extension grows in a direction which is parallel to the network segment being extended (wrong direction), or the extension doesn't reach any other network element within the maximum allowed extension, it is removed. Fig. 1 shows an example of correct extension.

4. Extreme points preserving line thinning

While in theory the line detection approach should provide single response, this was not observed in dermatological images, mainly because of the low contrast of the network and the discretization of the Gaussian kernels. So we introduced a one-pass raster thinning approach, which preserves the terminations. These are actually important for the diagnostic process, since they may point out the presence of abnormal lesion growth.

The thinning approach works by selectively eroding line points which match with exactly only one of the morphological masks of Fig. 3. These check for the presence of an "L" shaped point which is not an 8-connection between two different network segments. "T" shaped connections are then eroded with another set of masks (Fig. 4). This morphological filter is not well-behaved with respect to the line position, i.e. it moves the line to the rightmost position on every line, but this is not a problem for our application, since it is very uncommon to obtain lines which are wider than two pixels, and for these lines a position error is unavoidable, without going at sub-pixel level.

5. Line width estimation

To provide network line width estimation, the direction orthogonal to the line is employed. For this reason, junction points and closure points are not considered, since the gradient information is not reliable there, and may not match the real line curvature. For every network point found as before, the image levels are analyzed to look for the line edges. These edge points are found as the best fitting points, with respect to a 2-lines model of the luminance behavior, in both directions. The fitting error is computed as:

$$E(x) = \sum_{i=1}^{x-1} |I(i) - y_1| + \sum_{i=x+1}^{n} |I(i) - y_2| \qquad (9)$$

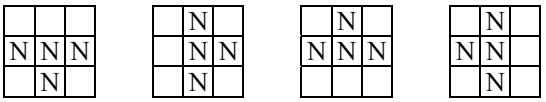

Figure 3. Morphological masks for network thinning at "T" points.

where $I(i)$ is the image data, i.e. the image intensity at point *i*, and y_1, y_2 the lines which define the model:

$$y_1 = I(0) + (I(x) - I(0))\frac{i}{x} \qquad (10)$$

$$y_2 = I(x) \qquad (11)$$

The intensity is computed by means of linear interpolation on the direction defined by the network orthogonal direction and the subpixel position of the network point.

This approach allows for the detection of lines width and can cope with the typical noise which is observable on this kind of images. The use of a linear model allows a fast search of the optimal position. Fig. 5 shows an example result of the luminance fitting on a specific network pattern.

6. Network properties extraction

After the network extraction and the line width estimation, the image is divided into 8 sectors oriented along the principal axes, in order to provide some statistics on the network characteristics of the whole lesion and of every eighth thereof. For each sector the number of meshes is counted with a straightforward 4-connection labeling, whereof the *circular* ones are counted, that is the ones with high area over squared perimeter, along with the number of unclosed terminations and the average line width. This information will then be collated with the clinical diagnosis and will allow describing the network behavior on these images.

7. Results

To test the ability of the algorithm in the detection of the network pattern, a set of 60 selected lesions was examined,

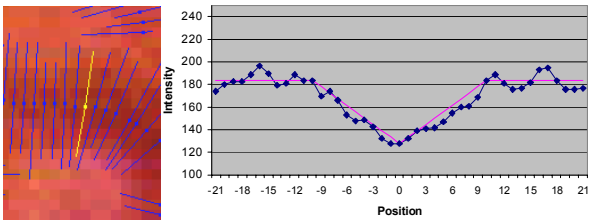

Figure 5. Result of width estimation algorithm on a network segment. The yellow line data are shown in the graph.

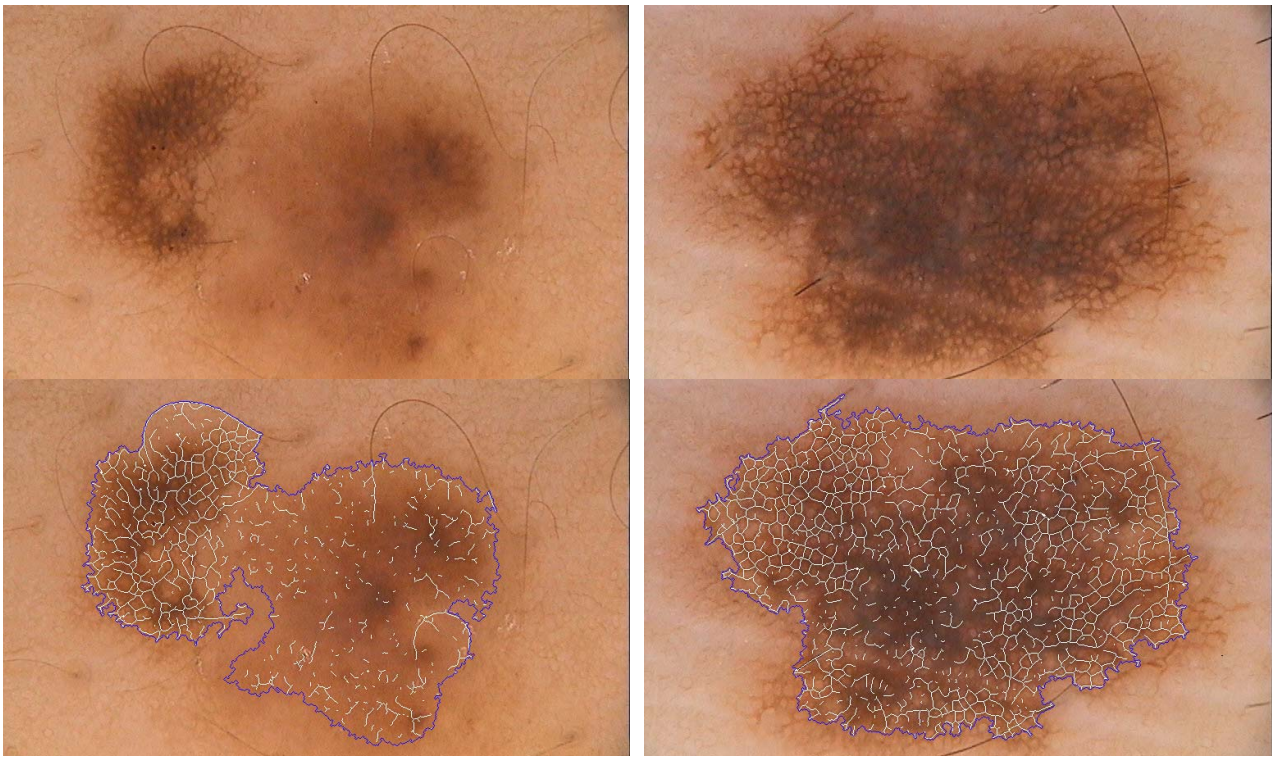

Figure 6. Example of two lesions images, showing a partial and complete network pattern.

selected from 3 classes (20 lesions per class) by the dermatologists: no network pattern, partial network pattern, complete network pattern. The aim was automatically identifying the presence or absence of the network pattern, for this reason two different features were employed: first of all the meshes were extracted as for the network properties extraction, then the network lines without a connection to a mesh were removed in order to keep only structurally significant elements. Every lesion was then characterized by the number of mashes and by the ratio between the number of network pixels and the lesion area. A lesion was selected as *no network* if it had less then T_M mashes and the network/lesion ratio was less then T_R.

The automatic threshold selection provided by the Fisher linear discriminant analysis keeps the threshold to a value which is usually slightly lower than ideal, but which correctly adapts to the different lesion examples of our tests. In this way, no false positives, 5 false negatives on the *partial network* class and 2 on the *complete network* class were detected, with an overall 88.3% network detection performance, without failed detections. The threshold was then lowered by an empirical 30%, for the lesions which were classified as presenting a network pattern, to obtain a denser detection and probably more significant network properties feature. The match between the clinical and computer extracted evaluations is still under analysis.

8. Conclusions

A full network pattern detection and characterization approach was described, which is able to cope with low contrast network patterns, does not need threshold selection, correctly closes different contrast meshes and produces 8-connected one-pixel wide network lines. A proposal for network characterization is under analysis.

References

[1] M. Anantha, R.H. Moss , W.V. Stoecker, Detection of pigment network in dermatoscopy images using texture analysis, *Comput Med Imaging Graph*, 28(5):225–34, 2004.

[2] C. Steger. An unbiased detector of curvilinear structures. *IEEE Trans Pattern Anal Machine Intell*, 20(2), Feb. 1998.

[3] M. G. Fleming, C. Steger, J. Zhang, J. Gao, A. B. Cognetta, I. Pollak, and C. R. Dyer. Techniques for a structural analysis of dermatoscopic imagery. *Comput Med Imaging Graph*, 22:375–389, 1998.

[4] Y. Deng, S. Kenney, M. Moore, and B. S. Manjunath. Peer group filtering and perceptual color image quantization. In *IEEE Int Symp Circuits Systems VLSI (ISCAS'99)*, volume 4, pages 21–24, Orlando, FL, June 1999.

[5] J. E. Bresenham. Algorithm for computer control of a digital plotter. *IBM Systems Journal*, 4(1):25–30, 1965.